binucleated, linear AuP_2 units; the ethylene groups in the dcpe bridges are twisted to give a Au-Au separation (2.936 Å) indicative of a metal-metal bonding interaction.[11] Each Au atom in **2** is bound to one chelating dcpe and one bridging dcpe, and each AuP_3 unit has a distorted trigonal planar geometry (Figure 1).[12] The **2** bridging unit is extended (Au-Au = 7.0501 Å); clearly, no Au-Au interaction is present.

The electronic absorption spectra of **1**, $[Au_2(dcpe)_3](PF_6)_2$ (**3**), and $[Au(dcpe)_2]PF_6$ (**4**) in acetonitrile solution are shown in Figure 2: **1** exhibits an intense band at 271 nm (ϵ = 10 000 M^{-1} cm^{-1}) and a weaker absorption at 320 nm (shoulder); **3** has a relatively weak absorption at 370 nm (ϵ = 300 M^{-1} cm^{-1} per AuP_3 unit); and the lowest energy absorption band in the spectrum of **4** is at 240 nm (ϵ = 35 000 M^{-1} cm^{-1}). Emission was observed for **1** as a solid at 77 K (λ_{max} = 489 nm), but not at room temperature; **3** emits both as a solid (λ_{max} = 501 nm) and in acetonitrile solution at room temperature (λ_{max} = 508 nm, τ = 21.1 (5) μs, ϕ = 0.80 (5)); **4** is nonemissive (solution or solid). The excitation spectrum of **3** confirms that absorption at 370 nm leads to emission (Figure 1).

The 370-nm absorption band in the spectrum of **3** is attributable to a $^1A_1 \rightarrow E'(^3E'')$ [$d\sigma^*(d_{xy}, d_{x^2-y^2}) \rightarrow p_z$] transition (for D_{3h} AuP_3).[13] Spin-orbit coupling splits the $^3E''$ state into A_1', A_2', E', and E'' levels, and the $^1A_1 \rightarrow E'$ transition is allowed. In the linear AuP_2 structure of **1**, the d_{xy}, $d_{x^2-y^2}$ level is no longer destabilized by σ(AuP) interactions, and the transitions from this level to p_z are expected to occur at much higher energy. The 271- and 320-nm bands in **1**, therefore, are logically due to transitions to $d\sigma^*(d_{z^2})p\sigma(p_z)$ singlet[1] and triplet states. Owing to its approximately tetrahedral AuP_4 structure, the valence p obitals of **4** are strongly σ antibonding. Accordingly, the lowest intense absorption band in **4** appears at a relatively high energy (240 nm).

Compound **3** is the first example of a gold complex containing an isolated Au^I unit that emits in solution at room temperature. This emission appears to be a property of the sterically protected AuP_3 monomeric unit.[12] Although there are a few reports of other three-coordinate gold(I) complexes,[14,15] most of the compounds are only stable as solids. In solution, facile ligand dissociation occurs to give the more stable linear $Au_2(L\text{-}L)_2$ complexes;[16] however, the trigonal planar geometry of each AuP_3 unit in **3** retains its integrity in solution.[9]

The large Stokes shift between $^1A_1 \rightarrow E'(^3E'')$ absorption (370 nm) and $^3E''$ emission (508 nm) indicates that a severe distortion of the AuP_3 structure occurs in the excited state. Depopulation of $d\sigma^*(d_{xy}, d_{x^2-y^2})$ should strengthen the Au-P bonds, thereby leading to a substantial contraction of the AuP_3 unit. Our results clearly show that long-lived Au^I excited states can be generated efficiently by irradiation of sterically protected Au^I monomeric units in solution. The oxidation-reduction chemistry of these excited states should be a rich area for exploration.

Acknowledgment. We thank Vinny Miskowski for several helpful discussions. T.M.M. acknowledges a National Science Foundation graduate fellowship and a fellowship from the Department of Education (Graduate Assistance in Areas of National Need). This work was supported by NSF Grant CHE8922067.

(11) Schaefer, W. P.; Marsh, R. E.; McCleskey, T. M.; Gray, H. B. Submitted for publication.
(12) Henling, L. M.; Flanagan, K. A.; McCleskey, T. M.; Gray, H. B. Manuscript in preparation.
(13) Jaw, H. R. C.; Savas, M. S.; Mason, W. R. *Inorg. Chem.* **1989**, *28*, 4366.
(14) Jones, G. C. H.; Jones, P. G.; Maddock, A. G.; Mays, M. J.; Vergnano, P. A.; Williams, A. F. *J. Chem. Soc., Dalton Trans.* **1977**, 1440.
(15) Usón, R.; Laguna, A.; Vicente, J.; Garcia, J.; Jones, P. G.; Sheldrick, G. M. *J. Chem. Soc., Dalton Trans.* **1981**, 655.
(16) Muetterties, E. L.; Alegranti, C. W. *J. Am. Chem. Soc.* **1970**, *92*, 4114.
(17) Contribution No. 8536.

Arthur Amos Noyes Laboratory[17]
California Institute of Technology
Pasadena, California 91125

T. Mark McCleskey
Harry B. Gray*

Received January 21, 1992

Articles

Contribution from the Department of Chemistry and Materials Science Center, Cornell University, Ithaca, New York 14853-1301, and Institut für Anorganische Chemie, Universität Hannover, Callinstrasse 9, W-3000 Hannover 1, Federal Republic of Germany

Distortions in the Structure of Calcium Carbide: A Theoretical Investigation

Jeffrey R. Long,[†,‡] Roald Hoffmann,*[,‡] and H.-Jürgen Meyer[§]

Received September 20, 1991

Recent ^{13}C NMR studies claim to have uncovered a flaw in the structure of CaC_2 as previously determined by powder neutron diffraction. It has been suggested that the apparent discrepancy between the ^{13}C NMR spectra and this structure is due to statistical disorder in the orientation of the C_2 dimer. Here, alternative CaC_2 structures in which the dicarbide unit has reoriented are explored by means of tight-binding extended Hückel band calculations. These calculations show the preferred orientation to be parallel to the *c*-axis, as found in the original structural refinements. However, they also reveal an extremely low-energy barrier for distortions in which the C_2 dimer rotates into a face of its octahedral Ca environment, and a somewhat higher barrier for distortions into an edge. The orbital interactions associated with the former distortion are examined in detail. Finally, a dicarbide-pairing distortion is considered and a fluxional model for the structure proposed.

Introduction

The CaC_2 structure adopted by most alkaline-earth carbides has long been cited in inorganic texts as the simplest example of a saltlike dicarbide.[1] The structure (Figure 1) consists of Ca^{2+} and C_2^{2-} ions arranged in a tetragonally distorted derivative of the NaCl structure, the distortion being due to the alignment of the C_2 dimers along the *c*-axis. This structure was determined from a powder neutron diffraction study, revealing that CaC_2 crystallizes at room temperature in the body-centered tetragonal system with space group $I4/mmm$ (D_{4h}^{17}) and unit cell parameters

† Present address: Department of Chemistry, Harvard University, Cambridge, MA 02138.
‡ Cornell University.
§ Universität Hannover.

(1) (a) Cotton, F. A. *Advanced Inorganic Chemistry*, 4th ed.; John Wiley & Sons: New York, 1980; pp 361-363. (b) Greenwood, N. N.; Earnshaw, A. *Chemistry of the Elements*; Pergamon Press: New York, 1984; pp 318-322. (c) Wells, A. F. *Structural Inorganic Chemistry*, 5th ed.; Clarendon Press: Oxford, U.K., 1984; pp 947-953.

0020-1669/92/1331-1734$03.00/0

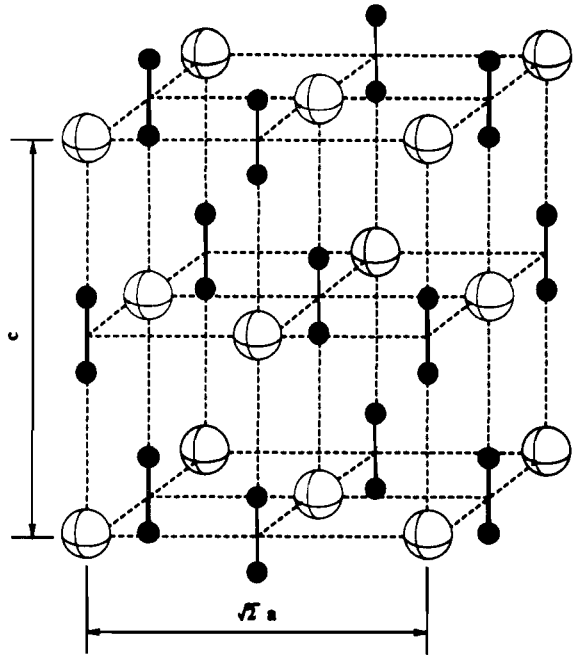

Figure 1. Structure of CaC_2. White spheres represent Ca atoms, and black spheres represent C atoms. The cell shown is double the conventional cell.

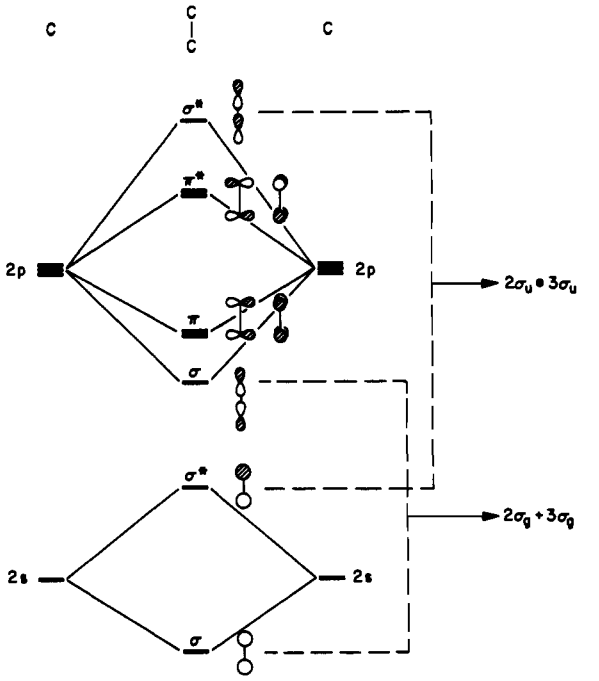

Figure 2. Formation of the valence orbitals of diatomic C_2. Mixing of orbitals with the same symmetry occurs as indicated.

$a = 3.89$ (1) Å, $c = 6.38$ (1) Å.[2] Notably, the dimeric C–C bond distance was determined to be 1.191 (9) Å, which is comparable to the distance of 1.205 Å found in acetylene.[3] A refinement of the structure by single-crystal X-ray diffraction has not been reported, presumably due to the difficulty of obtaining pure crystals of adequate size.

The validity of this structure has recently come into question. In particular, there is some doubt as to whether or not the C_2 dimers are actually parallel to the *c*-axis. Spectral broadening in the ^{13}C NMR spectra of CaC_2 seems to indicate a marked deviation of the carbon atoms from axial symmetry.[4] A plausible explanation for the differing conclusions drawn from the neutron diffraction data and the ^{13}C NMR spectra is that the C_2 dimers only statistically align along the *c*-axis. This same type of orientational disorder has been observed in many of the cyanides and hydrogen sulfides of the alkali metals.[5] Furthermore, there exist examples of rare-earth carbides containing C_2 dimers which are not axially situated.[1] In this paper we make use of extended Hückel[6] type band calculations in examining the energetics of several possible distortions of CaC_2 in which the dicarbide unit is rotated away from the *c*-axis.

Electronic Structure of Calcium Carbide

To begin, we need a clear understanding of the electronic structure of the undistorted CaC_2. In this section we shall see how this electronic structure evolves as we build the compound stepwise from its ionic components. First, the dicarbide unit will be formed by bringing together two C atoms and filling the orbitals with the appropriate number of electrons. The dicarbide sublattice of CaC_2 will then be constructed from these units, and finally, the Ca^{2+} ions will be introduced into the lattice.

The electronic structure of the C_2 unit with a bond length of 1.191 Å is that of a typical homonuclear diatomic molecule. The formation of its valence orbitals is diagrammed in Figure 2. There are two σ_g and two σ_u orbitals. These are first constructed as sums and differences of 2s and $2p_z$, respectively. But then s, p_z interaction must be included, leading to a well-understood mixing[7] and the formation of a strongly bonding $2\sigma_g$ orbital, two lone pair combinations ($2\sigma_u$ and $2\sigma_g$), and an antibonding $3\sigma_u$ orbital.

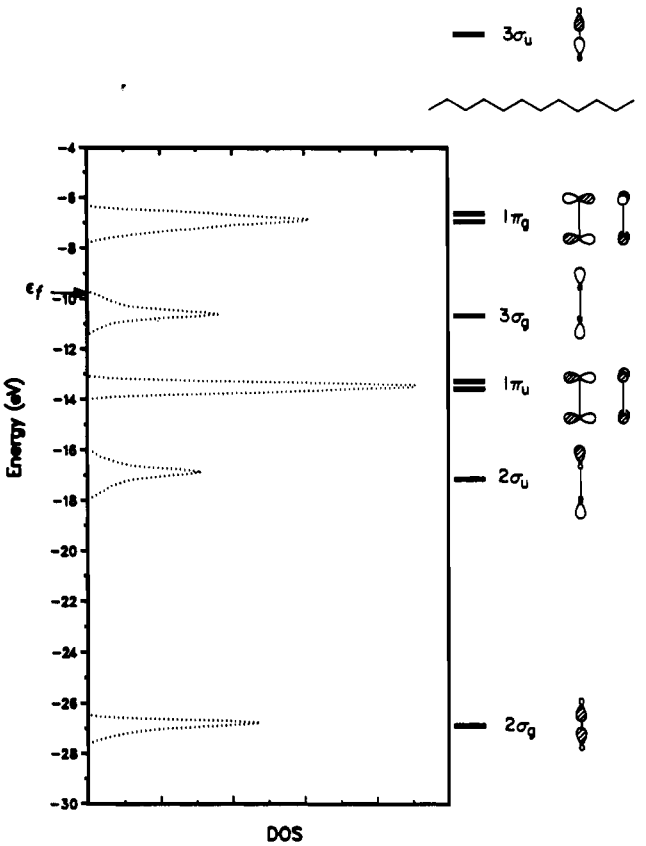

Figure 3. DOS of the C_2^{2-} sublattice compared with isolated C_2^{2-} energy levels. The $3\sigma_u$ level is off the energy scale.

(2) Atoji, M.; Medrud, R. C. *J. Chem. Phys.* **1959**, *31*, 332.
(3) Atoji, M. *J. Chem. Phys.* **1961**, *35*, 1950.
(4) (a) Wrackmeyer, B.; Horchler, K.; Sebald, A.; Merwin, L. H.; Ross, C. *Angew. Chem., Int. Ed. Engl.* **1990**, *29*, 807. (b) Duncan, T. M. *J. Chem. Phys.* **1989**, *28*, 2663.
(5) Parsonage, N. G.; Staveley, L. A. K. *Disorder in Crystals*; Clarendon Press: Oxford, U.K., 1978; pp 269–279.
(6) (a) Hoffmann, R. *J. Chem. Phys.* **1963**, *39*, 1397. (b) Hoffmann, R.; Lipscomb, W. N. *J. Chem. Phys.* **1962**, *37*, 2872. (c) Ammeter, J. H.; Burgi, H.-B.; Thibeault, J. C.; Hoffmann, R. *J. Am. Chem. Soc.* **1978**, *100*, 3686.
(7) Albright, T. A.; Burdett, J. K.; Whangbo, M. H. *Orbital Interactions in Chemistry*; John Wiley & Sons: New York, 1985; pp 77–80.

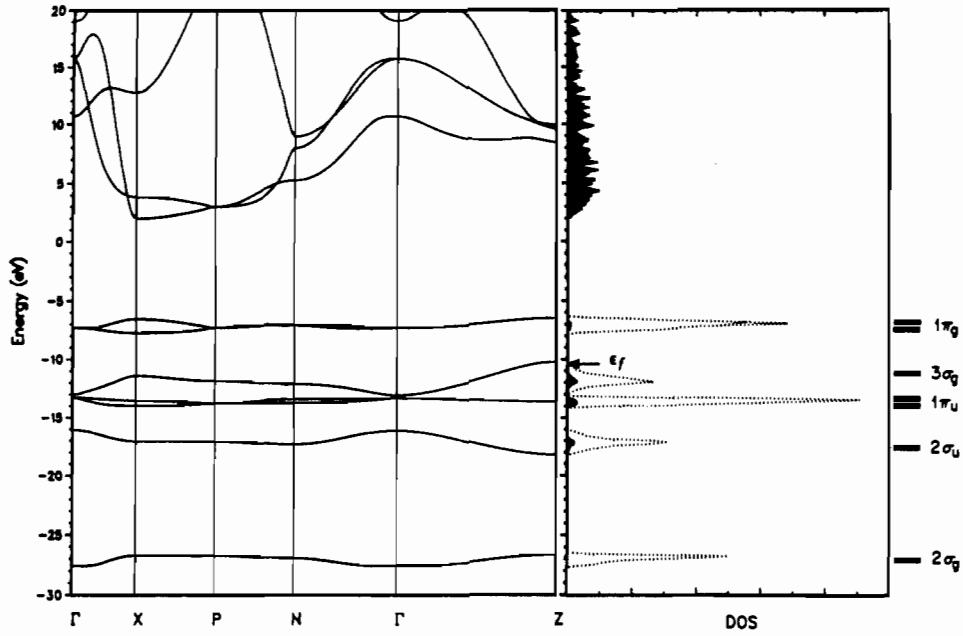

Figure 4. Band structure and DOS curve for CaC_2. The contribution of Ca to the DOS is shaded black. Isolated dicarbide energy levels are given on the right for comparison.

Schematically, these orbitals are shown at the right of Figure 3.

The 12-electron C_2 molecule has the ground-state configuration $(1\sigma_g)^2(1\sigma_u)^2(2\sigma_g)^2(2\sigma_u)^2(1\pi_u)^4$, $^1\Sigma_g^+$ with an equilibrium bond length of 1.24 Å.[8] The 14-electron C_2^{2-} unit is formed by simply adding two electrons, with the resulting configuration $(1\sigma_g)^2(1\sigma_u)^2(2\sigma_g)^2(2\sigma_u)^2(1\pi_u)^4(3\sigma_g)^2$. This unit is isoelectronic with N_2 and would therefore be expected to have an equilibrium bond length of less than 1.24 Å. From this point on, we will consider only valence electrons and refer to C_2^{2-} as having 10 electrons.

The discrete units are now brought together to form the dicarbide sublattice of CaC_2. As shown in Figure 3, this produces narrow energy bands centered at the discrete dicarbide energy levels.

The CaC_2 structure is completed with the addition of the Ca^{2+} ions. The resulting band structure is presented in Figure 4, along with the projected density of states (DOS)[9] and the corresponding energy levels for a discrete dicarbide unit. From the apparent band gap of ~2.3 eV we would predict CaC_2 to be a red insulator. In reality it is a colorless insulator,[1b] which corresponds to a band gap of at least 3 eV. This discrepancy may be a fault of the parameters chosen or may be inherent to the approximate MO method used.

Judging by the shifts of the C_2 levels upon Ca^{2+} incorporation, it is the $3\sigma_g$ level which is most affected by completion of the structure. Surprisingly, there is very little interaction between the dicarbide $1\pi_g$ orbitals and the equatorial Ca $4p_z$ orbitals which appear to be favorably positioned for overlap. Figure 5 shows schematically what happens. A measure of orbital interaction is given by the following perturbation expression.

$$\Delta E = \frac{|H_{ij}|^2}{E_i^\circ - E_j^\circ}$$

Thus, if two levels are far apart in energy, their interaction will be slight even if they have favorable overlap. This, combined with a slightly smaller overlap than might have been expected, seems to be the reason for the small dicarbide $1\pi_g$–Ca $4p_z$ interaction.

Two Principal Distortions

Taking a closer look at the environment of the dicarbide unit, we see that it has six Ca nearest neighbors forming an elongated octahedron around it. Thus, there are two different types of Ca atoms around each carbon atom: one axial Ca atom at a distance of 2.59 Å and four equatorial Ca atoms at a distance of 2.82 Å. We now consider rotations of the dicarbide unit within this quasi-octahedral environment. There exist two extremes in the orientation of the unit as it is rotated out of alignment with the c-axis. The first extreme is a rotation into a face of the octahedron, and the second is a rotation into a neighboring edge of the octahedron. These two distortions are illustrated and labeled in **1**; θ is the angle between the dicarbide axis and the c-axis.

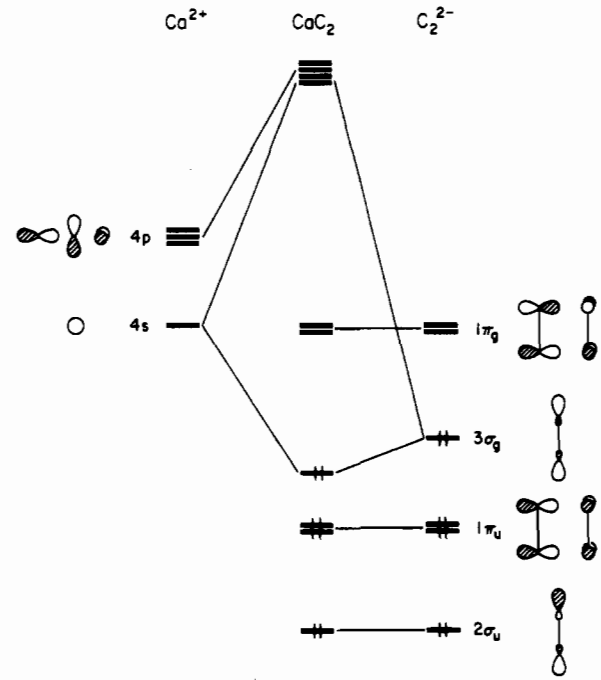

Figure 5. Interaction diagram for the introduction of Ca^{2+} ions into the dicarbide sublattice. Electrons fill through the $3\sigma_g$ band.

Extended Hückel calculations were performed on each distorted structure, varying the angle, θ, between 0 and 45°. Several trends were immediately noticeable. In each case, as θ increases, the Fermi level drops, reaching a minimum between 30 and 35°. As we shall see later, this does not necessarily correspond to a stabilization of the $3\sigma_g$ band. A plot of the total energy of the systems versus θ is shown in Figure 6. The total energy does not follow

(8) Herzberg, G. *Molecular Spectra and Molecular Structure*, 2nd ed.; D. Van Nostrand: New York, 1950; Vol. 1, pp 343, 513.
(9) Hoffmann, R. *Solids and Surfaces: A Chemist's View of Bonding in Extended Structures*; VCH Publishers: New York, 1988; pp 26–32.

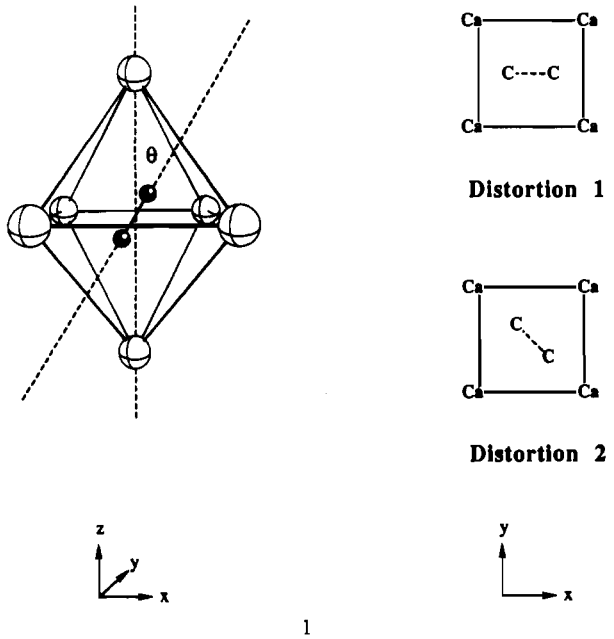

1

the Fermi level and is lowest at $\theta = 0°$, indicating that the undistorted structure is more stable than either of the two distorted structures. Distortions 1 and 2 both have maxima in total energy near $\theta = 35°$, with energy barriers of 0.09 and 0.23 eV, respectively. It should be noted that these maxima do not coincide with the points ($\theta = 23°$ and 18° for distortions 1 and 2, respectively) at which Ca_{eq}–C = Ca_{ax}–C.

Closer Examination of Distortion 1

Clearly, the less energetically disfavorable distortion is distortion 1, which we now look at in greater detail. Some insight is provided by comparing the band structure of the 35° distorted structure with that of the undistorted structure (Figure 7). While the effect is small, it may be seen in the $2\sigma_u$ and $3\sigma_g$ bands, whereas the $2\sigma_g$ (not shown), $1\pi_u$, and $1\pi_g$ bands are relatively unaffected by the distortion. From the integration of the contribution of Ca states to the DOS curves, we see that the amount of interaction of Ca with the dicarbide unit is greater for the distorted structure.

The $2\sigma_u$ and $3\sigma_g$ bands result from the lone pair combinations on the dicarbide unit. Their energy varies across the Brillouin zone, **2**, in mirrorlike fashion, one band moving up when the other

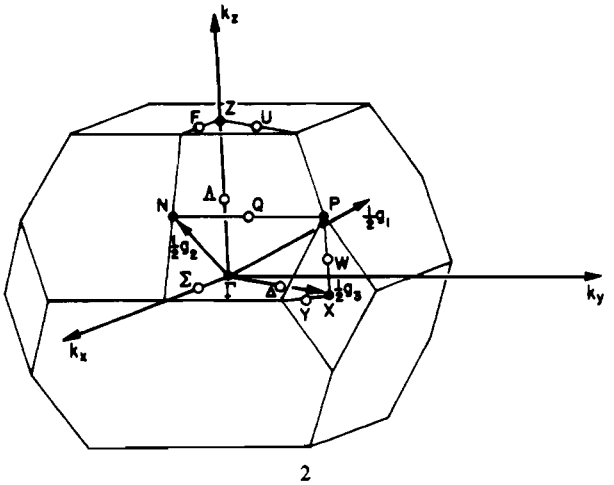

2

moves down. The most drastic changes occur along the lines between P and Γ. These lines are representative of a large portion of the Brillouin zone in which the $2\sigma_u$ band is stabilized and the $3\sigma_g$ band is destabilized as the dicarbide unit rotates away from the *c*-axis. This is precisely the region in which the horizontal mirror plane of symmetry is destroyed by the distortion, allowing the two orbitals to mix, and resulting in a typical 4-electron

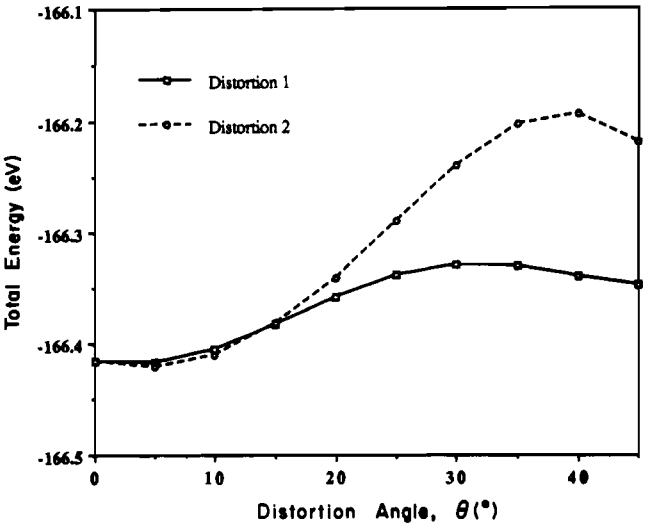

Figure 6. Total energy plot for distortions 1 and 2.

two-level repulsive interaction. As usual, the higher band ($3\sigma_g$) is destabilized more than the lower band ($2\sigma_u$) is stabilized, and the overall effect is an increase in the total energy.

Slightly countering this effect is the line from Γ to Z, which is representative of a much smaller portion of the Brillouin zone. Here the $3\sigma_g$ band favors the distortion, while the $2\sigma_u$ band does not. This can largely be explained by the change in overlap between the lone pairs on the dicarbide unit and the appropriate axial Ca orbitals. Between Γ and Z, the $3\sigma_g$ band consists of an interaction between the dicarbide $3\sigma_g$ orbitals and the axial Ca 4s orbitals, while the $2\sigma_u$ band consists of an interaction between the dicarbide $2\sigma_u$ orbitals and the axial Ca $4p_z$. As the bands run from Γ to Z, these interactions along the *c*-axis, **3**, change from

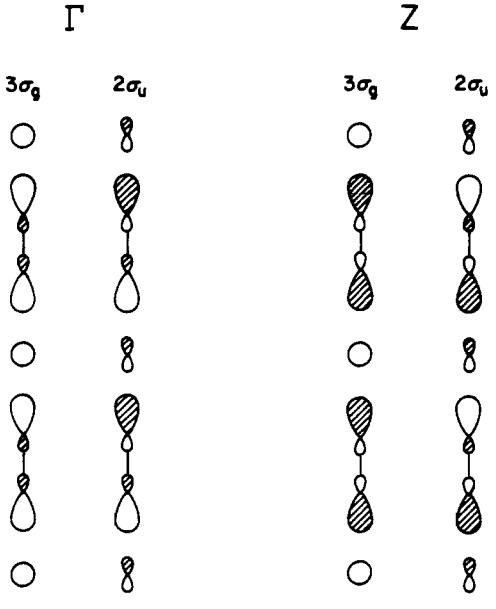

3

bonding in $3\sigma_g$ and antibonding in $2\sigma_u$ to antibonding in $3\sigma_g$ and bonding in $2\sigma_u$. When the dicarbide unit rotates away from the axial Ca atoms, there is less interaction, and the bands narrow.

Notably, the corresponding drop in energy of the $3\sigma_g$ band at Z is responsible for the lowering of the Fermi level for any distortion in which the dicarbide unit is rotated away from the axial position. The fact that Z represents so little of the Brillouin zone explains the lack of correlation between the total energy of the system and its Fermi level. Normally, in discrete molecules, the energy of the highest occupied molecular orbital (HOMO) determines the energy of the total system along some distortion coordinate. This is the frontier orbital hypothesis. By analogy one might expect the Fermi level to follow the total energy trend.

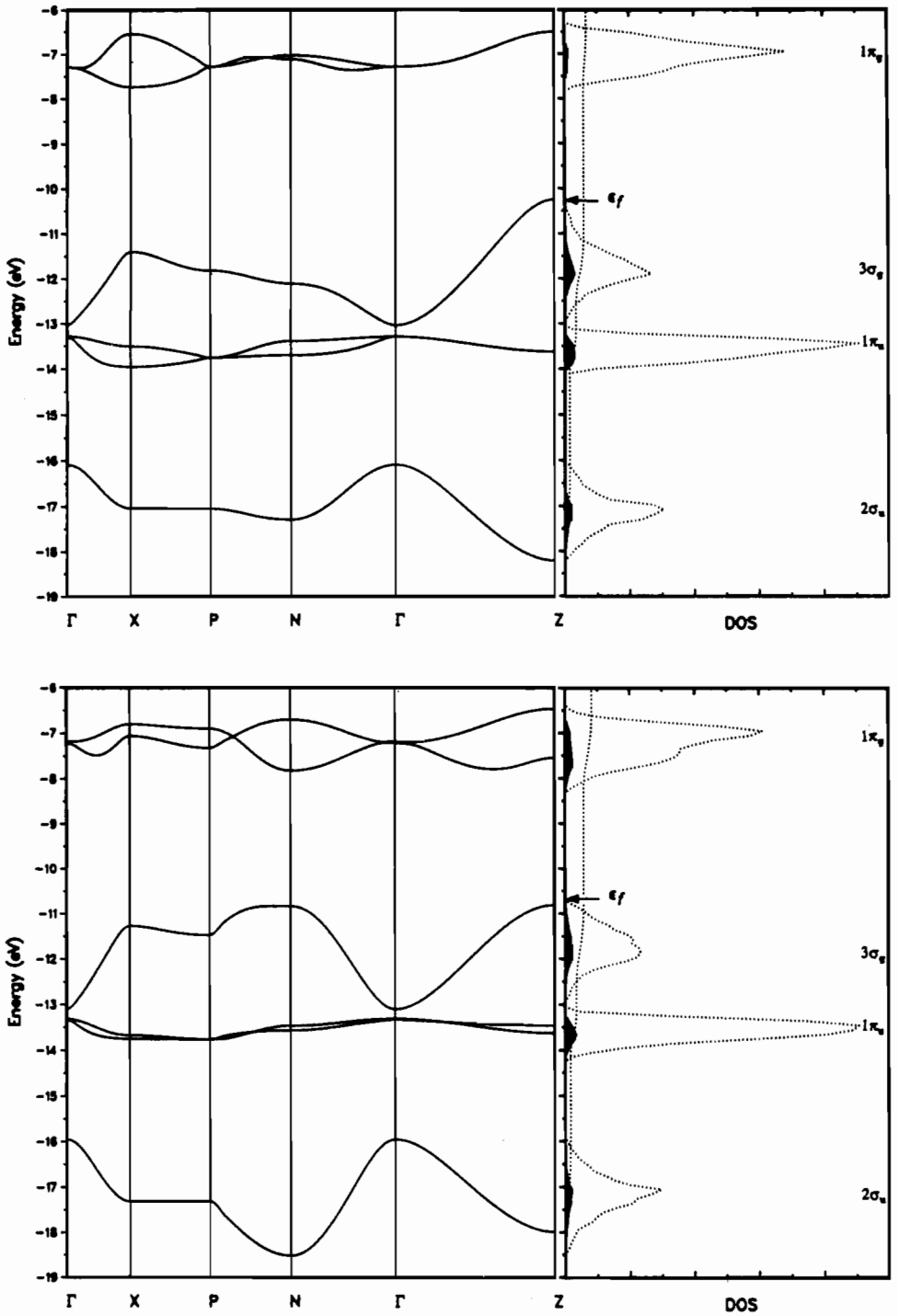

Figure 7. Band structure and DOS curves for undistorted CaC_2 (top) and distortion 1, $\theta = 35°$ (bottom). Integration is for the contribution of Ca, which is shaded black.

However, as exemplified here, the analogy can be a poor one, since not all states are represented equally in an energy band.

Figure 8 shows the crystal orbital overlap population (COOP)[10] curves for the two cases, which nicely illustrates the changes in overlap between C and the two different types of Ca. Immediately noticeable is the large increase in the amount of C–Ca bonding in the $1\pi_g$ band, which is responsible for the considerable stabilization of the band upon distortion. Thus, if we were studying a 14-electron system, we would see a large preference for the distorted structure. This fact has already been noted by Burdett and McLarnan in their investigation of the transition from the CaC_2 structure to the pyrite structure.[11]

(10) Hoffmann, R. *Angew. Chem., Int. Ed. Engl.* **1987**, *26*, 846.
(11) Burdett, J. K.; McLarnan, T. J. *Inorg. Chem.* **1982**, *21*, 1119.

Table I. Atomic Parameters Used in the Calculations

atom	orbital	H_{ii}, eV	ζ_1[a]
C	2s	−21.40	1.625
	2p	−11.40	1.625
Ca	4s	−7.00	1.200
	4p	−4.00	1.200

[a] Exponents in a double-ζ expansion of the Slater orbital.

A Pairing Distortion

We now turn our attention to longer range considerations. In distortion 1 the dicarbide units have all been tilted in the same direction. This is an oversimplification of the problem, which could not have produced the neutron diffraction results. We need, at the very least, some sort of disorder in the orientation of the

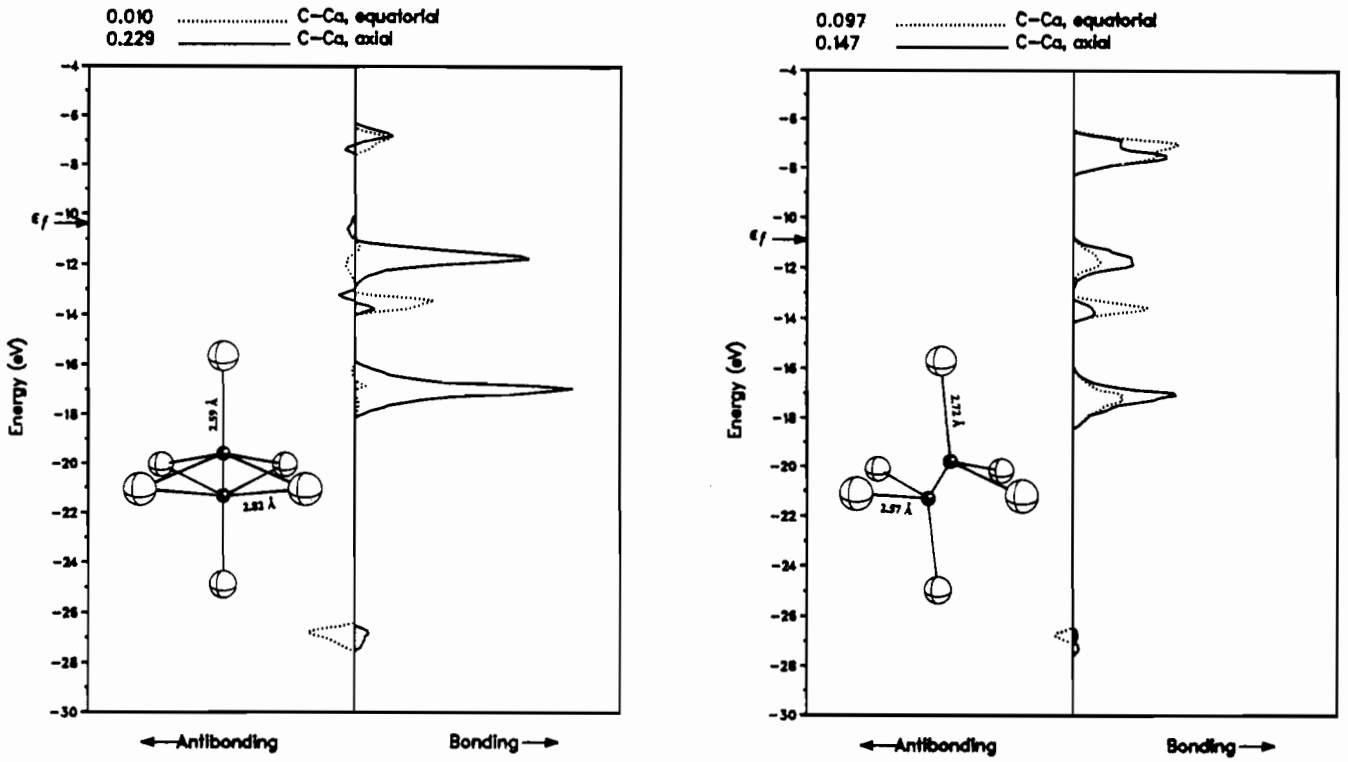

Figure 8. COOP curves for the two types of C–Ca bonds in undistorted CaC_2 (left) and distortion 1, $\theta = 35°$ (right). Total overlap populations are listed above each plot.

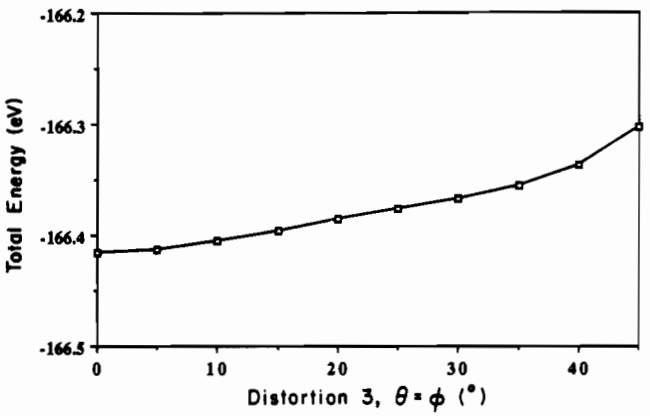

Figure 9. Total energy plot for distortion 3.

dicarbide unit that would statistically average to an axial dicarbide unit. The simplest such distortion (which we will refer to as distortion 3) creates a pairing of the C_2 dimers, and has the repeat unit shown in **4** with $\theta = \phi$.

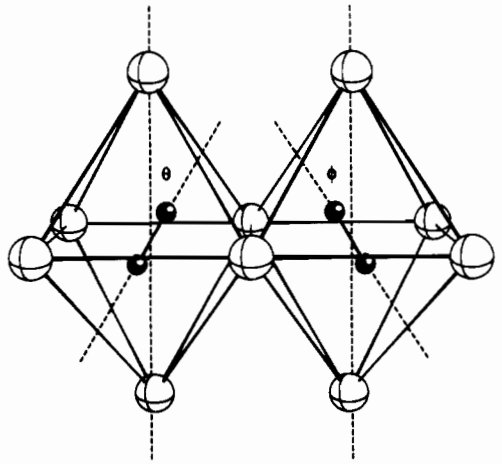

4, Distortion 3

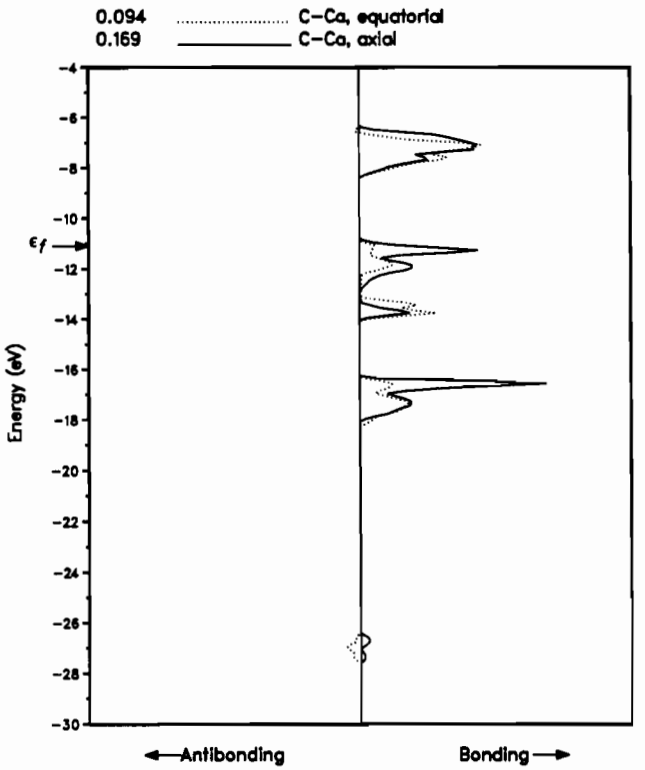

Figure 10. COOP curve for the two types of C–Ca bonds in distortion 3, $\theta = 35°$. Total overlap populations are listed at the top.

As expected, the results of distortion 3 are similar to those obtained in distortion 1. A plot of the variation of the total energy with the angle of rotation is presented in Figure 9. Significant is the fact that the rise in the total energy of the system is even smaller than that seen in distortion 1. The greater stability of this structure is not due to any favorable overlap between orbitals on neighboring dicarbide units but rather to an increase in the axial C–Ca bond strength. This is clear from the COOP curve of $\theta = 35°$ shown in Figure 10, which should be compared with

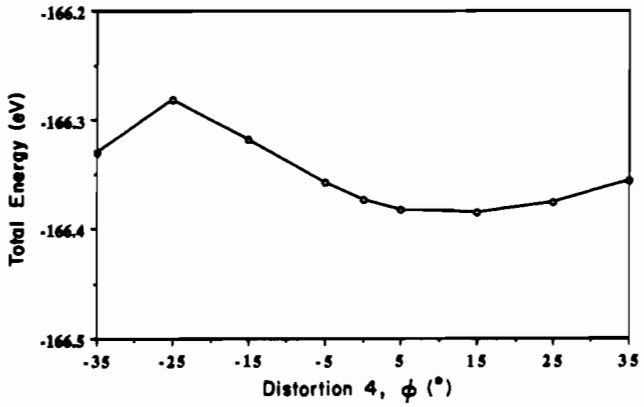

Figure 11. Total energy plot for distortion 4.

the COOP curve for distortion 1 (Figure 8 above).

Finally, we consider distortion 4, a transition from distortion 1 to distortion 3. Figure 11 shows a plot of the total energy for distortion 4 in which θ is kept constant at 35° while ϕ is varied between −35 and +35° (see **4**). The energy barrier for this rotation is small (~0.1 eV); however, the energy minimum is substantially offset from 35°. As the dicarbide unit rotates beyond $\phi = 0°$, an unfavorable overlap between the $2\sigma_u$ orbitals on the paired dicarbides arises. Hence, the minimum in energy near $\phi = 15°$ is a result of the fine tuning of interactions between C and Ca, and the interaction between dicarbide units. Interestingly, since the point at $\phi = 0°$ is not a minimum, the distortion of a single unit initates the distortion of its neighbors. Thus, if one dicarbide unit is provided with enough energy to rotate, then the distortion can, to some extent, propagate through the solid.

Concluding Remarks

As we have seen, the original structure of CaC_2 is indeed the most stable one, at least with our approximate molecular orbital calculations. However, the barrier for rotation of the C_2 dimer away from the *c*-axis is extremely small; significant population of rotated geometries is possible at room temperature. Therefore, at higher temperatures we might expect a very different structure, and indeed, at least four metastable phases of CaC_2 have been reported.[12] From our analyses of these distortions, we propose a fluxional model in which the dicarbide unit, while preferring a time-averaged alignment with the *c*-axis, spends some part of its time distorted in the direction of a face of its coordination octahedron and the least amount of its time distorted toward an edge. A similar model has been proposed for NaCN at room temperature in a single-crystal neutron diffraction study.[13] Such a study on CaC_2 would resolve this issue but awaits successful growth of sizeable pure crystals.

Appendix

An extended Hückel tight-binding approach was employed in all of the calculations. The atomic parameters used were taken from previous work[6a,14] and are tabulated in Table I. A set of 125 k-points was used for calculations of average properties. The band structures were calculated at 6 k-points along each line between special points in the Brillouin zone.

Acknowledgment. This work was supported by the National Science Foundation through Research Grants CHE-8912070 and DMR-8818558.

Registry No. CaC_2, 75-20-7.

(12) (a) Bredig, M. A. *Z. Anorg. Allg. Chem.* **1961**, *310*, 338. (b) Vannerberg, N.-G. *Acta Chem. Scand.* **1962**, *15*, 769. (c) Vannerberg, N.-G. *Acta Chem. Scand.* **1961**, *16*, 1212.
(13) Rowe, R. M.; Hinks, D. G.; Price, D. L.; Susman, S.; Rush, J. J. *J. Chem. Phys.* **1973**, *58*, 2039.
(14) Zheng, C.; Hoffmann, R. *J. Am. Chem. Soc.* **1986**, *108*, 3078.

Contribution from the Department of Synthetic Chemistry, Faculty of Engineering, Kyoto University, Kyoto 606, Japan

Electronic Structures of Dative Metal–Metal Bonds: Ab Initio Molecular Orbital Calculations of $(OC)_5Os$–$M(CO)_5$ (M = W, Cr) in Comparison with $(OC)_5M$–$M(CO)_5$ (M = Re, Mn)

H. Nakatsuji,* M. Hada, and A. Kawashima

Received November 8, 1991

The nature of the metal–metal bonds in the binuclear complexes $(OC)_5Os$–$M(CO)_5$ (M = W, Cr) is studied by ab initio MO calculations and compared with that of the covalent metal–metal bonds in $(OC)_5M$–$M(CO)_5$ (M = Re, Mn). We confirm that the former complexes have a dative metal–metal bond, as suggested experimentally. The $Os(CO)_5$ fragment, which has an 18-electron configuration, acts as an electron donor to the $M(CO)_5$ (M = W, Cr) fragments, which have 16-electron configurations, to form stable binuclear complexes. The highest occupied σ-orbital of $Os(CO)_5$ and the lowest unoccupied σ-orbital of $M(CO)_5$ (M = W, Cr) interact and form the metal–metal dative σ-bonding orbital. The electron transfer occurs not only around the two metals, but also within each fragment, including CO ligands. The calculated bond formation energies are 20.9 and 7.7 kcal/mol for $(OC)_5Os$–$W(CO)_5$ and $(OC)_5Os$–$Cr(CO)_5$, respectively. They are smaller than those of the covalent complexes $(OC)_5M$–$M(CO)_5$ (M = Re, Mn), 54.0 kcal/mol for M = Re and 32.5 kcal/mol for M = Mn. However, the bond lengths and the force constants of the Os–W and Os–Cr bonds are comparable with those of the Re–Re and Mn–Mn bonds. The calculated distances are 3.04, 2.86, 2.98, and 2.86 Å and force constants are 1.08, 0.79, 1.53, and 0.66 mdyn/Å for Os–W, Os–Cr, Re–Re, and Mn–Mn, respectively. These values reasonably agree with the experimental values. The smallness of the bond formation energy in $(OC)_5Os$–$M(CO)_5$ (M = W, Cr) is mainly due to a large geometrical relaxation of the $Os(CO)_5$ fragment in the course of the dissociation. In $(OC)_5Os$–$M(CO)_5$, the HOMO is a metal–metal σ-bonding orbital for M = Cr, but metal–ligand π-bonding orbital for M = W. The metal–metal σ-bond is stronger in $(OC)_5Os$–$W(CO)_5$ than in $(OC)_5Os$–$Cr(CO)_5$, and different reactivities are expected for electrophiles.

Introduction

The possibility that a neutral 18-electron transition-metal compound can act as a two-electron donor to the 16-electron transition-metal compound to form a dative metal–metal bond has been suggested for a long time. The first such report appears to be that of Hock and Mills for $Fe_2(\mu\text{-}CO)(CO)_5(C_4R_4)$.[1] However, two alternative electron-counting schemes are possible for this complex, so that this metal–metal bond can also be re-

(1) Hock, A. A.; Mills, O. S. *Acta Crystallogr.* **1961**, *14*, 139.

0020-1669/92/1331-1740$03.00/0